ACKNOWLEDGMENTS

We thank Catherine Zurcher for skillful technical assistance with the immunochemical methods.

SUPPLEMENTARY MATERIAL AVAILABLE

Four tables containing amino acid compositions of CNBr peptides and their subpeptides of *Amphioxus* SCP I and SCP II and seven figures showing the elution profile of CNBr peptides of SCP II and HPLC separation patterns for CNBr peptides in fractions I, III, and IV, of SCP I and SCP II, and of mixtures of tryptic peptides (20 pages). Ordering information is given on any current masthead page.

Registry No. Ca, 7440-70-2; Mg, 7439-95-4; SCPI, 101858-44-0; SCPII, 101858-45-1.

REFERENCES

Collins, J. H., Johnson, J. D., & Szent-Györgyi, A. G. (1983) *Biochemistry 22*, 341–345.
Cox, J. A., & Stein, E. A. (1981) *Biochemistry 20*, 5430–5436.
Cox, J. A., Wnuk, W., & Stein, E. A. (1976) *Biochemistry 15*, 2613–2618.
Gariepy, J., & Hodges, R. S. (1983) *FEBS Lett. 160*, 1–6.
Habeeb, A. F. S. A. (1972) *Methods Enzymol. 25*, 457–464.
Haiech, J., & Sallantin, J. (1985) *Biochimie 67*, 555–560.
Harboe, N., & Ingild, A. (1973) in *A Manual of Quantitative Immunoelectrophoresis* (Axelsen, N. H., Kroll, J., & Weeks, B., Eds.) p 161, Universitetsforlaget, Oslo.
Kobayashi, T., Takasaki, Y., Takagi, T., & Konishi, K. (1984) *Eur. J. Biochem. 144*, 401–408.
Kohler, L., Cox, J. A., & Stein, E. A. (1978) *Mol. Cell. Biochem. 20*, 85–93.
Laemmli, U. K. (1970) *Nature (London) 227*, 680.
Moews, P. C., & Kretsinger, R. H. (1975) *J. Mol. Biol. 91*, 201–228.
Takagi, T., & Konishi, K. (1984) *J. Biochem. (Tokyo) 95*, 1603–1615.
Takagi, T., Kobayashi, T., & Konishi, K. (1984) *Biochim. Biophys. Acta 787*, 252–257.
Tarr, G. E. (1977) *Methods Enzymol. 47*, 335–357.
Wnuk, W., & Jauregui-Adell, J. (1983) *Eur. J. Biochem. 131*, 177–182.
Wnuk, W., Cox, J. A., & Stein, E. A. (1982) in *Calcium and Cell Function* (Cheung, W. Y., Ed.) Vol. II, pp 243–278, Academic, New York.

Anomalous Asymmetric Kinetics of Human Red Cell Hexose Transfer: Role of Cytosolic Adenosine 5′-Triphosphate†

Anthony Carruthers

Department of Biochemistry, University of Massachusetts Medical Center, Worcester, Massachusetts 01605

Received November 18, 1985; Revised Manuscript Received February 5, 1986

ABSTRACT: Cytosolic adenosine 5′-triphosphate (ATP) modifies the properties of human red cell sugar transport. This interaction has been examined by analysis of substrate-induced sugar transporter intrinsic fluorescence quenching and by determination of Michaelis and velocity constants for D-glucose transport in red cell ghosts and inside-out vesicles lacking and containing ATP. When excited at 295 nm, human erythrocyte ghosts stripped of peripheral proteins display an emission spectrum characterized by a scattering peak and a single emission peak centered at about 333 nm. Addition of sugar transport substrate or cytochalasin B and phloretin (sugar transport inhibitors) reduces emission peak height by 10% and 5%, respectively. Cytochalasin B induced quenching is a simple saturable phenomenon with an apparent K_d (app K_d) of 60 nM and a capacity of 1.4 nmol of sites/mg of membrane protein. Quenching by D-glucose (and other transported sugars) is characterized by at least two (high and low) app K_d parameters. Inhibitor studies indicate that these sites correspond to sugar efflux and influx sites, respectively, and that both sites can exist simultaneously. ATP induces quenching of stripped ghost fluorescence with half-maximal effects at 20–30 μM ATP. ATP reduces the low app K_d and increases the high app K_d for sugar-induced fluorescence quenching. D-Glucose transport in intact red cells is asymmetric (K_m and V_{max} for influx < K_m and V_{max} for efflux). In addition, two operational K_m parameters for efflux are detected in zero- and infinite-trans efflux conditions. Protein-mediated sugar transport in ghosts and inside-out vesicles (IOVs) is symmetric with respect to K_m and V_{max} for entry and exit, and only one K_m for exit is detected. Addition of millimolar levels of ATP to the interior of ghosts or to the exterior of IOVs restores both transport asymmetry and two operational K_m parameters for native efflux. A model for red cell hexose transport is proposed in which ATP modifies the catalytic properties of the transport system. This model mimics the behavior of the sugar transport systems of intact cells, ghosts, and inside-out vesicles.

In spite of extensive study, the properties of human red cell sugar transport "defy simple description" (Naftalin & Roselaar, 1985). The properties of erythrocyte hexose transfer appear to be consistent with Widdas' original suggestion (the mobile carrier hypothesis; Widdas, 1952) that a single sugar binding/transport site is alternately accessible at each surface of the plasma membrane (Krupka & Deves, 1981; Gorga & Lienhard, 1981). Nevertheless, the observation of asymmetry in Michaelis and velocity constants for sugar influx and efflux and the discovery of two operational sugar transport sites at

† This work was supported in part by National Science Foundation Grant DCB-8510876, National Institutes of Health Grant R01 AM36081-01, and NIH Biomedical Research Grant S07 RR05712.

0006-2960/86/0425-3592$01.50/0

the inner surface of the plasma membrane have resulted in rejection of simple symmetric and asymmetric carrier models for red cell sugar transport [for reviews, see Naftalin & Holman (1977) and Widdas (1980)]. Apparently, the transport mechanism is more complex than has been allowed for to date, or those transport measurements demonstrating anomalous red cell sugar transport behavior are theoretically or technically flawed.

A large body of evidence supports the validity of previous transport determinations. Sugar transport asymmetry and the presence of two operational sugar efflux sites have been demonstrated by a variety of experimental methods (Harris, 1963; Sen & Widdas, 1962; Hankin et al., 1972; Ginsberg & Stein, 1975; Foster et al., 1979; Baker & Naftalin, 1979; Carruthers & Melchior, 1983a, 1985), and the Michaelis and velocity constants derived from either initial rate or integrated rate kinetic analysis of these experiments are in substantial agreement. In addition, recent criticisms of integrated and initial rate analyses of these transport data (due to a suggested differential transport of α and β anomers of D-glucose; Gorga & Lienhard, 1981; Wheeler & Hinkle, 1985) have proven to be without experimental basis (Weiser et al., 1983; Carruthers & Melchior, 1985).

Naftalin and Holman (1977) and Baker and Naftalin (1979) approached this problem from a different perspective. They proposed a model for sugar transport in which the experimental properties of transport were governed by factors extrinsic to the transport system. Their model proposed that sugar fluxes are symmetric but that nonspecific binding of cytosolic hexose and water to hemoglobin results in the underestimation and overestimation of intracellular sugar concentrations in influx and efflux experiments, respectively. The net effect is experimental kinetic asymmetry and the presence of two operational sugar efflux sites [see Naftalin & Holman (1977)]. Sugar transport measurements made with substantially hemoglobin-free red cell ghosts support this hypothesis [Jung et al., 1971; Benes et al., 1972; Taverna & Langdon, 1973; Carruthers & Melchior, 1983a; Speizer et al., 1985; note, however, Challiss et al. (1980) found no effect of 95% hemoglobin removal on sugar transport]. In addition, cytochalasin B sensitive transport in inside-out red cell vesicles (IOVs,[1] where in principle, the cytoplasmic surface of the plasma membrane faces an infinite dilution of hemoglobin) is symmetric (Carruthers & Melchior, 1983a; Taverna & Langdon, 1973). However, the study of Carruthers and Melchior (1983a) suggested that the loss of intracellular, low molecular weight factors rather than hemoglobin was responsible for this effect.

Weiser et al. (1983) have demonstrated that the K_m for protein-mediated exchange transport in freshly drawn cells is almost doubled after 8 weeks of cold storage. Jacquez (1983) has reported that ATP can modulate the red cell sugar transport system. It has since been demonstrated (Carruthers, 1986) that the direct interaction of ATP with the otherwise simple, symmetric sugar transport mechanism of IOVs reduces both K_m and V_{max} for sugar efflux from red cell inside-out vesicles. Moreover, direct studies of the effects of ATP upon the intrinsic tryptophan fluorescence of purified band 4.5 protein (the sugar transporter) indicated that the transporter was subject to modulation by ATP via interaction with a single nucleotide binding site on the transporter (Carruthers, 1986).

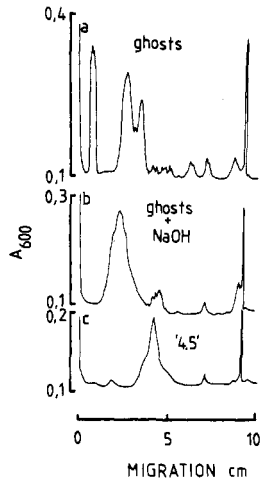

FIGURE 1: Scans of the electrophoretic patterns of (a) white ghosts (15 μg), (b) stripped (NaOH-treated) ghosts (9 μg), and (c) "purified" band 4.5 protein (6 μg). Membranes were run on 10% polyacrylamide gels. Dried gels were scanned at 600 nm with a Beckman DU-8 spectrophotometer in the gel scanning mode.

This study examines the effects of ATP and a number of other nucleotides on red cell sugar transport and the intrinsic tryptophan fluorescence of red cell ghosts stripped of peripheral proteins. The results of this investigation further support the view that erythrocyte hexose transfer is subject to physiologic modulation by ATP.

Materials and Methods

Materials. Freshly outdated, whole human blood was obtained from the University of Massachusetts Medical Center Blood Bank.

Solutions. Tris medium consisted of 50 mM Tris-HCl/0.2 mM EDTA adjusted to pH 7.4 by using 1 M Tris base. KCl medium contained 150 mM KCl/5 mM Tris-HCl/0.2 mM EDTA, pH 7.4. Lysis medium contained 5 mM Tris-HCl/0.2 mM EDTA at pH 8. Alkaline lysis medium contained 5 mM Tris-HCl/0.2 mM EDTA adjusted to pH 12 by using 1 M NaOH. Vesiculation medium contained 10 mM Tris-HCl/4 mM EDTA at pH 7.5.

Preparation of Red Cell Ghosts and Inside-Out Vesicles (IOVs). Ghosts and IOVs were formed as described previously (Carruthers & Melchior, 1983a).

Preparation of Stripped Ghosts. White ghosts were prepared from washed human red cells by hypotonic lysis in 40 volumes of ice-cold lysis medium followed by repeated washing in ice-cold lysis medium (Carruthers & Melchior, 1983a). When the membranes had a pearly white appearance, they were collected by centrifugation and then exposed to 10 volumes of ice-cold alkaline lysis medium for 20 s. The membranes were washed in 10 volumes of Tris medium, collected by centrifugation, and then repeatedly washed in Tris medium until the pH of the supernatant was 7.4 (normally three washes). The membranes were frozen rapidly and thawed 3 times to increase their permeability to sugars and then stored at −25 °C in Tris medium at a concentration of 2 mg of membrane protein/mL. These membranes are nominally free of all peripheral membrane proteins (see Figure 1) and are highly permeable to D-glucose (equilibration with 200 mM D-glucose was achieved within 5–15 s).

[1] Abbreviations: IOVs, inside-out red cell membrane vesicles; ATP, adenosine 5′-triphosphate; AMP, adenosine 5′-monophosphate; ADP, adenosine 5′-diphosphate; AMP-CPP, adenosine 5′-(α,β-methylenetriphosphate); AMP-PCP, adenosine 5′-(β,γ-methylenetriphosphate); Ap_4A, P^1,P^4-di(adenosine-5′) tetraphosphate; EDTA, ethylenediaminetetraacetic acid; Tris-HCl, tris(hydroxymethyl)aminomethane hydrochloride; kDa, kilodalton(s); NATA, *N*-acetyltryptophanamide; app K_d, apparent K_d; DIDS, 4,4′-diisothiocyano-2,2′-stilbenedisulfonic acid; SITS, 5-(acetylamino)-2-[2-(4-isothiocyanato-2-sulfophenyl)ethenyl]benzenesulfonic acid disodium salt; RBCs, red blood cells.

Fluorescence Measurements. Fluorescence measurements were performed at 23 ± 1 °C by using a Farrand MK 2 spectrofluorometer with excitation at 295 nm and an emission bandwidth of 10 nm. Stripped membranes (200 μg of protein in 100 μL) were added to 2 mL of Tris medium. Sugars and transport inhibitors (stock concentrations, pH 7.4, in Tris medium) were injected into the cuvette from above. The contents of the cuvette were constantly stirred with a Spectrocell Inc. cuvette stirrer. In all instances, steady-state emission levels were reached within 5–20 s following addition of ligand and (provided the excitation bandwidth was 2.5–5 nm) remained stable for up to 15 min. When the excitation bandwidth was increased to 10 nm, the emission of stripped membranes decayed monoexponentially with a half-time of some 14 min. This decay of emission has been ascribed to photolysis of tryptophan residues (Appleman & Lienhard, 1985). Initially, all quenching data (measured as the reduced emission at 333 nm with excitation at 295 nm) were corrected for dilution and nonspecific effects by titration either against L-glucose in sugar experiments or against carrier (ethanol or dimethyl sulfoxide) plus cytochalasin D or E in cytochalasin B experiments. With L-glucose, mannitol, and cytochalasins D and E (agents that fail to interact with the sugar transporter of red cells), the dilution-corrected emission was within 98–100% of control emission levels. This provided a convenient correction procedure in these experiments. In studies with nucleotides and phloretin, alternative correction procedures were adopted. Steady-state fluorescence quenching levels are subject to the following systematic errors: (1) the inner filter effect (attenuation of the exciting light by added ligand); (2) ligand-induced changes in the fluorescence spectral shape or position; (3) changes in the refractive index of solutions upon addition of ligand; (4) absorption spectral changes; (5) fluorescence reabsorption by ligand. Sugars, nucleotides, and inhibitors induce a shift in the emission peak of stripped membranes to shorter wavelengths by 1–2 nm. The necessary correction for this shift was less than 1% in 180 mM D-glucose and 50 μM cytochalasin B (assuming no quenching). Changes in the transporter's absorbance spectrum by added ligand were assessed by analysis of the absorption spectra of stripped membranes in the absence and presence of the highest concentrations of added ligand. The difference spectra of ligand/buffer/membranes − ligand/buffer were essentially identical (in position, shape, and absorbance) to the absorption spectrum of transporter in buffer alone. Refractive index corrections range from zero to n^2 (Chen, 1981). The correction in 180 mM D-glucose is approximately 2%. Initially, inner filter effects were corrected as suggested by Parker (1968) where

$$\frac{F_{cor}}{F} = \frac{2.203A(d2 - d1)}{10^{-Ad1} - 10^{-Ad2}}$$

A is the total absorbance at the excitation wavelength, and $d1$ and $d2$ refer to the geometry of the observed volume. Fluorescence reabsorption was most significant in studies with phloretin where the absorption spectrum of phloretin overlaps the emission spectrum of stripped membranes. At first, the obtained "quenching" data (corrected for dilution and inner filter effects) were corrected by calculation of the absorption coefficient of each ligand (at each concentration used) followed by applying Lambert's law to calculate the original intensity of emission. Finally, an empirical approach to the problem of correction was adopted [see Torikata et al. (1979)]. The fluorescence of a standard (*N*-acetyltryptophanamide, NATA) was measured as a function of added ligand. The optical densities of NATA and stripped membranes were the same. After correction for the above-mentioned systematic errors, the emission of NATA in the presence of sugars, inhibitors, and nucleotides over the range of concentrations employed in this study was within 98–100% of control emission. This indicates that NATA is not quenched by these ligands. Stripped membrane data were then corrected for nonquenching errors by using NATA data. The results obtained were not systematically different from those obtained by application of the initial, calculated corrections.

All results reported here have been corrected as described above. Absorption measurements were made by using a Beckman DU-8 spectrophotometer.

Transport Determinations. Zero-trans efflux, infinite-cis exit, and infinite-cis entry in ghosts and IOVs at 20 °C were monitored as described previously (Carruthers & Melchior, 1983a, 1985). The loading D-glucose concentration for zero-trans efflux and infinite-cis efflux experiments was 60 mM. Turbidimetry was used to monitor sugar exits (Carruthers & Melchior, 1983a,b, 1985).

All transport determinations were made in the presence and absence of cytochalasin B (10 μM) and phloretin (50 μM), competitive inhibitors of sugar efflux and influx, respectively (Krupka & Deves, 1981). Preparations in which inhibited fluxes (transport in the presence of inhibitors) were greater than 2.5% of control fluxes were discarded.

Analytical Methods. Protein assays were as described by Lowry et al. (1951). Sodium dodecyl sulfate–polyacrylamide gel electrophoresis was carried out on 10% gels as described previously (Carruthers & Melchior, 1984).

Calculation of Michaelis–Menten Parameters from Fluorescence Quenching Data. Two methods were employed. In instances where Eadie/Scatchard plots indicated the data were described by a single set of Michaelis–Menten parameters, these parameters were obtained by fitting the raw data to the Michaelis–Menten equation using weighted nonlinear regression with "robust" methods for the modification of residuals (Duggleby, 1981). In instances where Eadie/Scatchard plots indicated at least two sets of Michaelis–Menten parameters, an iterative procedure of successive approximation (Spears et al., 1971) was employed to obtain Michaelis constants for two components of substrate binding.

RESULTS

Fluorescence Measurements with Stripped Membranes. Alkali-treated red cell ghost membranes contain membrane protein bands 3, 4.5, 7, and PAS 1-3. Band 3 is the anion transport protein, and band 4.5 contains the glucose transport protein (80–86%; Batt et al., 1976; Kasahara & Hinkle, 1977; Hanahan & Jacquez, 1978; Baldwin et al., 1982; Carruthers & Melchior, 1984) and nucleoside transporter (4%; Jarvis & Young, 1981). It is also probable that the (Na, K)-ATPase, Ca-ATPase, Ca-sensitive K channel, and a variety of other electrolyte and nonelectrolyte transport proteins are present in these membranes. While band 4.5 represents only some 10% of the total protein content of stripped ghost membranes (Baldwin et al., 1979), it was of interest to determine whether the well-documented, substrate-induced intrinsic tryptophan fluorescence quenching of purified sugar transporter (band 4.5 protein; Gorga & Lienhard, 1982) could also be detected in stripped membranes containing a variety of proteins.

When excited at 295 nm, stripped ghost membranes display a fluorescence emission spectrum characterized by two major peaks—one at 295 nm due to scattering of the excitation beam and a second centered at 334 nm that presumably results from tryptophan fluorescence of membrane protein (Burstein et al.,

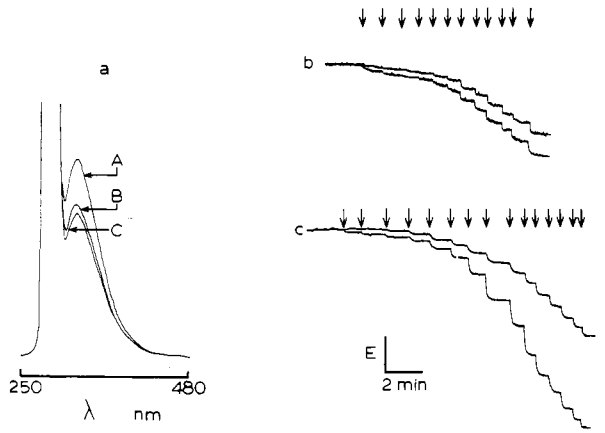

FIGURE 2: Fluorescence quenching of stripped ghosts by D-glucose and cytochalasin B. (a) Emission spectra of stripped ghosts (200 μg of membrane protein/2.1 mL of Tris medium) in the absence (A) and presence of 3 μM cytochalasin B (B) or 132 mM D-glucose (C). Excitation wavelength, 295 nm. (b) Effects of cytochalasin B (+ dimethyl sulfoxide) and cytochalasin D (+ dimethyl sulfoxide) on emission (at 333 nm) of stripped ghosts (initial concentration, 200 μg of protein in 2.1 mL) with excitation at 295 nm. The upper trace shows the "quenching" produced by successive additions (shown by the arrows) of cytochalasin D (100 μM in Tris medium + 0.1% dimethyl sulfoxide). The volumes added were 1, 1, 1, 1, 6, 10, 20, 40, 50, 70, 70, and 80 μL. Essentially identical results were obtained by using NATA in place of stripped membrane ghosts and cytochalasin B rather than cytochalasin D as the added ligand. The lower trace is an analogous experiment in which identical additions of cytochalasin B (100 μM) in 0.1% dimethyl sulfoxide (Tris medium) to stripped membranes were made. The difference between the two records is taken as cytochalasin B induced quenching. The cuvette was stirred constantly with a Spectrocell Micro-stirrer. Temperature, 23 °C. Time base as indicated. The y axis represents emission at 333 nm. Sensitivity identical for cytochalasin D + dimethyl sulfoxide and cytochalasin B + dimethyl sulfoxide records. (c) Effects of L- and D-glucose on emission (at 333 nm) of stripped ghosts (initial concentration, 200 μg of protein in 2.1 mL). The upper trace shows the quenching produced by successive additions (shown by the arrows) of L-glucose (1 M) in Tris medium. The volumes added were 0.5, 0.5, 1, 1, 1, 1, 6, 10, 20, 40, 50, 70, 70, 70, and 70 μL. The lower trace is an analogous experiment in which identical additions of D-glucose (1 M in Tris medium) were made. Time base and temperature as in (b). The y axis is identical for both L- and D-glucose records but is of higher (2-fold) sensitivity than in (b).

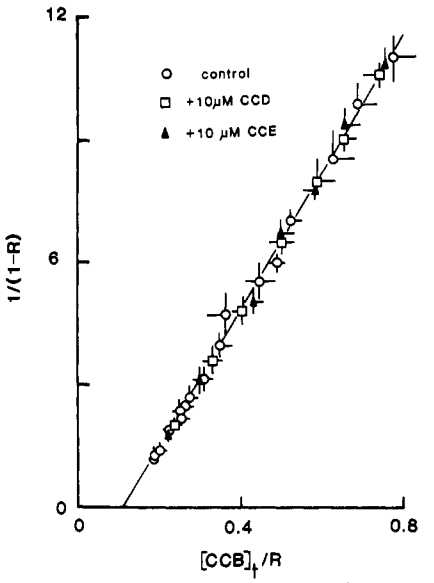

FIGURE 3: Cytochalasin B (CCB) induced fluorescence quenching of stripped ghosts. Emission at 333 nm was measured with excitation at 295 nm. Initial protein concentration, 200 μg in 2.1 mL. Ordinate, $1/(1-R)$; abscissa, total cytochalasin B concentration/R (μM). R is the fractional saturation of the preparation by cytochalasin B. The equation for such a plot is $K_d = C_L(1/R - 1) - nC_E(1 - R)$ where C_L is the total cytochalasin B concentration, C_E the total cytochalasin B binding protein concentration, and n the stoichiometry of cytochalasin B binding to the protein. The advantage of such a plot is that R is readily measured and nC_E may be read directly from the x intercept. The experiments (16 in total) were performed by making successive additions of cytochalasin B [and parallel, control cytochalasin D (CCD) + dimethyl sulfoxide runs] until the quenching produced by cytochalasin B specifically did not increase upon further additions of cytochalasin B (normally at 5–10 μM cytochalasin B). R was calculated as observed quenching/saturated quenching. The slope of such a plot is 1/app K_d, and the x intercept gives n[cytochalasin B binding sites] where n is the stoichiometry of binding of cytochalasin B to acceptor proteins. Three sets of data are shown: control (○) and cytochalasin B induced quenching in the presence of 10 μM cytochalasin D (□) or 10 μM cytochalasin E (▲) (CCE). Data are shown as mean ± 1 SE. Number of individual experiments per point, three or more. The data fall on a single straight line ($R > 0.99$) with an app K_d for cytochalasin B binding of 60 ± 5 nM and an x intercept of 0.11 ± 0.01 μM. Assuming a stoichiometry for cytochalasin B binding to band 4.5 protein of 0.86 (Baldwin et al., 1982; Carruthers, 1985) and that the average molecular mass of band 4.5 is 55 kDa, this corresponds to a concentration of cytochalasin B binding sites of 1.4 nmol/mg of stripped ghost membrane protein (8% of total protein).

1973). Upon addition of the sugar transport inhibitor cytochalasin B, or the transport substrate D-glucose, the emission peak at 334 nm is shifted by 3 nm toward shorter wavelengths, and the peak height is reduced by about 18% (see Figure 2a). When corrected for systematic errors, the maximum specific quenching produced by cytochalasin B is considerably less (6%, Figure 2b). Similarly, when D-glucose data are corrected for possible nonspecific effects and sample dilution by titration of membranes against L-glucose, the maximum specific quenching by D-glucose is also reduced (to 10%, Figure 2c).

Kinetic analysis of corrected cytochalasin B data indicates a single population of cytochalasin B binding sites with an app K_d of 0.06 ± 0.005 μM (Figure 3). The extrapolated concentration of cytochalasin B binding sites under these conditions is 0.11 ± 0.01 μM. Assuming that fluorescence quenching is associated with cytochalasin B binding to band 4.5 protein (a 55-kDa protein) and a molar stoichiometry of binding of 0.86 [see Baldwin et al. (1982) and Carruthers (1985)], this means that 200 μg of stripped ghost membrane protein contains 15 μg of band 4.5 protein or 1.4 nmol of sites/mg of membrane protein—an estimate in close agreement with that of Gorga and Lienhard (1981) (1.8 nmol of sites/mg of membrane protein). Cytochalasin B induced stripped membrane fluorescence quenching is unaffected by cytochalasin D or E (Figure 3), confirming that the glucose carrier independent cytochalasin binding sites (classes II and III; Lin & Snyder, 1977; Jung & Rampal, 1977) had been lost upon alkali treatment of red cell ghosts. The concentration dependence of D-glucose-induced fluorescence quenching of stripped membrane ghosts confirms the presence of at least two D-glucose binding sites (Figure 4). Analysis of these data indicates the presence of both a high-affinity, low app K_d site (K_1) of 1.33 ± 0.12 mM and a low-affinity, high app K_d site

Table I: Binding Constants for Sugar-Induced Fluorescence Quenching[a]

sugar	low app K_d (mM)	high app K_d (mM)
D-glucose	1.33 ± 0.12	39.0 ± 4.2
2-deoxy-D-glucose	1.80 ± 0.21	43.7 ± 3.5
3-*O*-methylglucose	2.62 ± 0.17	98.7 ± 5.9
galactose	6.83 ± 2.14	73.6 ± 6.3
maltose	2.90 ± 0.10	107.0 ± 6.0
ethylidene glucose	0.69 ± 0.04	27.1 ± 0.3

[a] Number of experiments per condition, three or more.

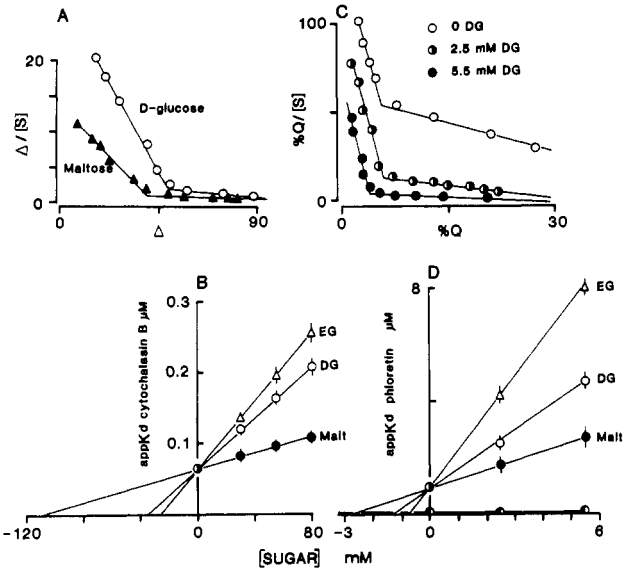

FIGURE 4: Effects of sugars and phloretin on stripped ghost membrane fluorescence. (A) Eadie/Scatchard plots of D-glucose- and maltose-induced fluorescence quenching. Ordinate, decrease in emission/sugar concentration; abscissa, decrease in emission. Two sets of data are shown: D-glucose- (○) and maltose-induced (▲) quenching. The presence of two slopes for each data set indicates at least two components of quenching by each sugar. The app K_d for sugar binding in a single-component system is given by $K_d = -1/\text{slope}$. Using the method of successive approximation (Spears et al., 1971), we obtain for D-glucose $K_1 = 1.33 \pm 0.12$ nM and $K_2 = 39 \pm 4.2$ nM. For maltose, we obtain $K_1 = 2.9 \pm 0.1$ mM and $K_2 = 107 \pm 6$ mM. Each point represents the mean of at least three separate determinations. The emission scale was normalized between separate runs by using 180 mM sugar as a standard reference point. (B) Effects of D-glucose (DG), ethylidene glucose (EG), and maltose (Malt) on the app K_d for cytochalasin B induced fluorescence quenching. Ordinate, app K_d for cytochalasin B binding (μM); abscissa, sugar concentration (mM). The lines drawn through the points were calculated by linear regression ($R > 0.95$ in each instance). The x intercept corresponds to −app K_i for competitive inhibition of cytochalasin B binding by the sugars. These values are 37.9 ± 6.7, 28 ± 2.1, and 112 ± 9.8 mM for DG, EG, and Malt, respectively. Individual points are shown as mean ± 1 SE. Number of experiments per point, three or more. (C) Phloretin-induced fluorescence quenching of stripped ghosts and the effects of D-glucose (DG). Ordinate, percent quenching/phloretin concentration; abscissa, percent quenching by phloretin. Data are shown for quenching in the absence (○) and presence of 2.5 (◑) or 5 (●) mM D-glucose. Each point is shown as mean ± SE. Number of experiments per point, three or more. The presence of at least two slopes in these Eadie/Scatchard plots indicates at least two components of quenching. The method of successive approximation gives the following: control, $K_1 = 0.1 \pm 0.02$ μM and $K_2 = 1.0 \pm 0.1$ μM; +2.5 mM DG, $K_1 = 0.11 \pm 0.02$ μM and $K_2 = 2.2 \pm 0.3$ μM; +5.5 mM DG, $K_1 = 0.09 \pm 0.01$ μM and $K_2 = 4.5 \pm 0.7$ μM. (D) Effects of D-glucose (DG), ethylidene glucose (EG), and maltose (Malt) on the app K_d for phloretin-induced quenching of stripped ghost fluorescence. Ordinate, app K_d of phloretin-induced quenching in micromolar; abscissa as in (B). The lines drawn through the points were calculated by linear regression ($R > 0.96$ in each instance). The x intercept corresponds to −app K_i for competitive inhibition of phloretin binding by the sugars. These values are 1.26 ± 0.3, 0.72 ± 0.04, and 2.8 ± 0.4 mM for DG, EG, and Malt, respectively. The low app K_d for phloretin-induced quenching was unaffected by D-glucose, ethylidene glucose, and maltose (◐). Individual points are shown as mean ± SE. Number of experiments per point, three or more.

(K_h) of 39 ± 4.2 mM. Similar results were obtained with D-galactose, 2-deoxy-D-glucose, and 3-*O*-methylglucose (Table I). The sugars maltose and ethylidene glucose (sugars that bind to the transporters but, for steric reasons, are not transported) also induce two-component, saturable membrane fluorescence quenching (Table I).

Both low and high app K_d sugar binding sites appear to be associated with the hexose transport system. D-Glucose increases the app K_d for cytochalasin B induced fluorescence quenching with an app K_i of 37.9 ± 6.7 mM (Figure 4), suggesting that the low-affinity sugar binding site is the site of competition between D-glucose and cytochalasin B. Maltose and ethylidene glucose also increase the app K_d for cytochalasin B induced fluorescence quenching with app K_i values of 112 ± 9.8 and 28 ± 2.1 mM, respectively (Figure 4). These app K_i parameters are indistinguishable from K_h for D-glucose, maltose, and ethylidene glucose induced fluorescence quenching (Table I) and agree with the study of Sogin and Hinkle (1980) where the app K_i values for D-glucose and maltose inhibition of [^{3}H]cytochalasin B binding to purified band 4.5 were 43 and 120 mM, respectively. Similarly, Gorga and Lienhard (1981) report app K_i values for D-glucose and ethylidene glucose inhibition of cytochalasin B binding to stripped ghost membranes of 59 and 26 mM, respectively. These findings suggest strongly that the high K_d site (K_h) detected in sugar-induced fluorescence quenching measurements is analogous to the native, endofacial site of competition between D-glucose and cytochalasin B for binding to the transport system (Krupka & Deves, 1981; Gorga & Lienhard, 1981) and the high K_m site for sugar efflux in red cells (Widdas, 1980). Phloretin is a competitive and noncompetitive inhibitor of sugar influx and efflux, respectively, in human red cells (Krupka & Deves, 1981), indicating that it reacts with the external orientation of the sugar transport molecule. Phloretin also induces quenching of stripped membrane fluorescence (Figure 4). Two saturable components of quenching are detected in Eadie/Scatchard plots—one with an app K_d of 0.1 μM and a second with an app K_d of 1 μM. D-Glucose, maltose, and ethylidene glucose increase the high app K_d for phloretin-induced fluorescence quenching with app K_i values of 1.26 ± 0.3, 2.8 ± 0.4, and 0.72 ± 0.04 mM, respectively. The low app K_d for quenching is unaffected by D-glucose (Figure 4). These data suggest strongly that the high app K_d phloretin binding site detected in fluorescence quenching studies is associated with the sugar transporter and that the high-affinity sugar binding site, K_1, is associated with the external orientation of the sugar transport molecule.

Table II: Effects of Ouabain and Anion Transport Inhibitors on Fluorescence Quenching[a]

	app K_d			
agent	control	+SITS[b]	+DIDS[b]	+ouabain[c]
D-glucose (mM), K_1	1.3 ± 0.1	1.2 ± 0.1	1.5 ± 0.3	1.4 ± 0.2
D-glucose (mM), K_h	39 ± 4	41 ± 3	37 ± 6	40 ± 4
cytochalasin B (μM)	0.06 ± 0.01	0.06 ± 0.01	0.05 ± 0.01	0.06 ± 0.01
ATP (μM)	26 ± 2	27 ± 4	28 ± 3	39 ± 4

[a] Number of experiments per condition, three or more. [b] SITS and DIDS concentration, 5 μM. [c] Ouabain concentration, 10 μM.

ATP and a variety of other nucleotides also induce fluorescence quenching of stripped membranes (Figure 5). Quenching is normally completed within 20 s. ATP modifies the ability of D-glucose to induce fluorescence quenching of stripped membranes; 0.5 mM ATP decreases (K_1) 1.96-fold to 0.68 ± 0.04 mM and increases (K_h) 1.91-fold to 74.5 ± 5.8 mM ($n = 4$; see Figure 6). This effect on sugar-induced quenching is reversed by washing membranes in ATP-free Tris medium.

Fluorescence quenching dose responses to sugars and cy-

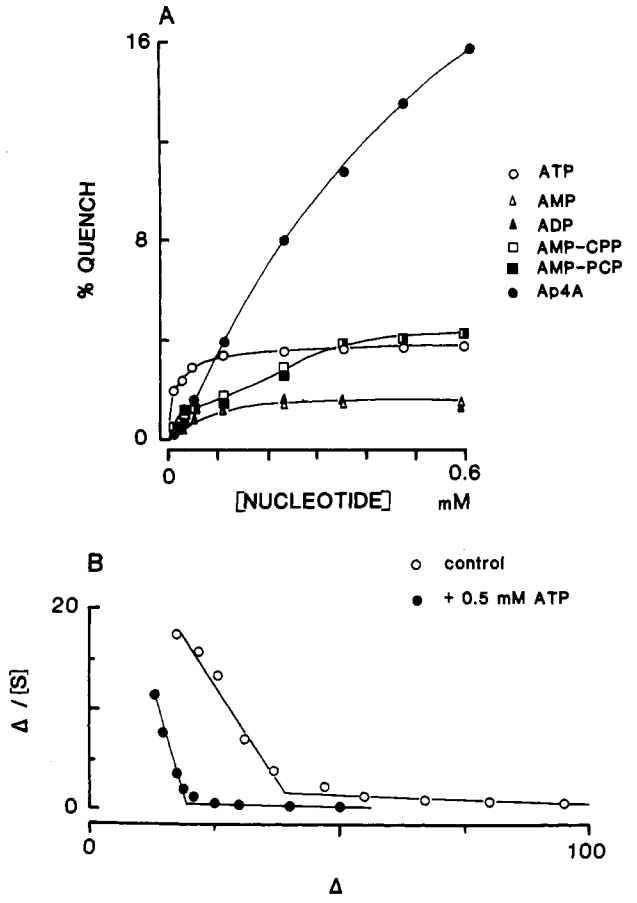

FIGURE 5: Effects of adenosine nucleotides on fluorescence of stripped ghosts. (A) Effects of ATP (○), AMP (△), ADP (▲), the nonmetabolizable ATP analogue AMP-PCP (■), the metabolizable ATP analogue AMP-CPP (□), and Ap_4A (●) on stripped ghost fluorescence. Ordinate, percent quenching; abscissa, nucleotide concentration (mM). The curves drawn through the ATP and AMP/ADP data each correspond to a section of a single rectangular hyperbola with app K_d values of 20 and 67 μM and maximum quenching of 3.9% and 1.4%, respectively. The curves drawn through the remaining data points are of no theoretical significance. (B) Effects of ATP (0.5 mM) on fluorescence quenching of stripped ghosts by D-glucose. Ordinate, decrease in emission/[D-glucose]; abscissa, decrease in emission. D-Glucose data are shown in the absence (○) and presence (●) of 0.5 mM ATP. The method of successive approximation gives K_1 and K_2 parameters for D-glucose binding of 1.33 ± 0.08 mM and 39 ± 3 mM, respectively, in the absence of ATP and 0.68 ■ 0.04 mM and 74.5 ± 5.8 mM in the presence of ATP.

tochalasin B were not significantly affected by the anion transport inhibitors DIDS and SITS (5 μM) or by the (Na, K)-ATPase inhibitor ouabain (10 μM; Table II). Ouabain did, however, cause a 1.5-fold increase in the app K_d for ATP-induced quenching of stripped ghosts. At this point, it is uncertain whether this reflects a direct action on the Na pump or the ability of ouabain to interact with the transporter [ouabain has been shown to mimic the action of ATP depletion on sugar transport in muscle and other tissues; see, for example, Baker & Carruthers (1983)]. The anion transport inhibitors induce fluorescence quenching of stripped membranes although the effects of both inhibitors are indistinguishable. Two components of quenching are detected, one with an app K_d of 17.4 ± 1.6 μM and maximum quenching (Q_m) of 12.3 ± 1.1% and a second with an app K_d of 0.86 ± 0.8 μM and a Q_m of 3.6 ± 0.2%.

Effect of Nucleotides on Sugar Transport in Inside-Out Red Cell Vesicles and Red Cell Ghosts. Two types of red cell preparations have been employed in this study—the red cell ghost and the inside-out vesicle (IOV). The reasons for

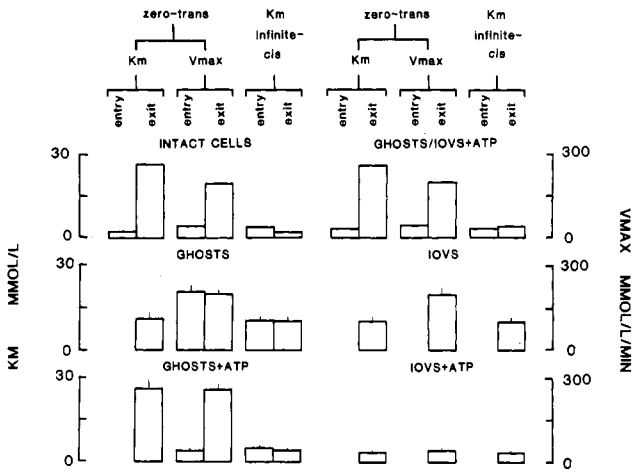

FIGURE 6: Effects of ATP on K_m and V_{max} for D-glucose transport in red cell ghosts and inside-out vesicles (IOVs). Ordinate, K_m (mM) and V_{max} [mmol (L of cell water)$^{-1}$ min^{-1}]. Three types of flux determinations were made: (A) measurements of K_m and V_{max} for sugar efflux into sugar-free medium (zero-trans efflux); (B) measurements of K_m for sugar efflux into saturating glucose medium and V_{max} for entry into sugar-free cells (infinite-cis entry); (C) measurements of K_m for influx into cells containing saturating levels of D-glucose and V_{max} for exit into sugar-free medium (infinite-cis exit). These experiments are indicated above the bar graphs. Intact red cell data were obtained from literature values (Naftalin & Holman, 1977). Two sets of ghosts data are presented—control data and data from ghosts formed containing 4 mM ATP. Two sets of IOV data are also presented—control IOVs and IOVs preincubated and injected into assay media containing 1 mM ATP. IOV V_{max} data have been "adjusted" for the 3-fold greater surface area of 1 L of IOVs (see Results). Ghost + ATP and IOV + ATP have been combined (see upper right panel) by assuming that "adjusted" efflux from IOVs is equivalent to influx in ghosts. Data are presented as mean ± SE. Number of experiments per condition, six or more. Temperature, 20 °C.

working with IOVs are 2-fold. (1) It is possible to expose the normally endofacial surface of the plasma membrane to predefined media which, during the course of an experiment, remain essentially unchanged. (2) Zero-trans influx measurements in red cells (influx into cells lacking sugar) are technically more difficult than the corresponding efflux procedure (efflux into sugar-free medium). Thus, an estimate of the zero-trans influx parameters may be obtained more readily from zero-trans efflux measurements made with IOVs. The average IOV diameter was determined by electron microscopy to be 2.5 μM. IOV size was not affected significantly by ATP. Assuming IOVs are spherical, this means that the surface area of that number of IOVs containing 1 L of intravesicular water is approximately 3-fold greater than the area of RBCs containing 1 L of water (10^{13} cells). As the V_{max} for transport is expressed as moles of sugar per liter of cell water per unit time, this means that estimates of the V_{max} for transport in IOVs will be 3-fold greater than the V_{max} in ghosts under identical experimental conditions. This was found experimentally, and all V_{max} data in IOVs have been "adjusted" for this area factor to facilitate comparison of V_{max} data between ghosts and IOVs.

It has previously been established that ATP reduced both K_m and V_{max} for zero-trans efflux from IOVs (Carruthers, 1986). ATP was half-maximally effective at 50 μM and could not be substituted for by AMP, ADP, AMP-CPP, or AMP-PCP. Figure 6 summarizes a large number of zero-trans efflux and infinite-cis determinations made by using both ghosts and IOVs. The infinite-cis entry procedure provides estimates of V_{max} for net entry and K_m for exit (into saturating glucose medium), and the infinite-cis exit procedure measures V_{max}

for exit and K_m for entry. In some experiments, ATP was incorporated into ghosts at 4 mM and transport determinations with IOVs were made in solutions containing 1 mM ATP. Also included in this figure are intact red cell data [for a review, see Naftalin & Holman (1977)]. The major findings are as follows: (1) Asymmetry in V_{max} and K_m parameters for zero-trans fluxes is lost in ghosts. Moreover, the two operational K_m parameters for efflux from intact cells are no longer detected. (2) Incorporation of ATP into ghosts restores not only the asymmetry in V_{max} parameters for zero-trans fluxes but also the two operational K_m parameters characteristic of transport in intact cells. (3) K_m and the adjusted V_{max} for zero-trans efflux from IOVs are indistinguishable from K_m and V_{max} from both zero-trans influx and efflux in ATP-free ghosts. The K_m for influx into IOVs containing 60 mM sugar is identical with the K_m for both infinite-cis entry and exit in ghosts. (4) ATP reduces both K_m and V_{max} for zero-trans efflux from IOVs and reduces K_m for infinite-cis exit. Assuming that an influx procedure made with ghosts is analogous to an efflux procedure made with IOVs, these results demonstrate that ATP essentially restores the properties of intact cells to both ghosts and IOVs.

ATP reduces the K_m for D-glucose exit from IOVs within 5 min of exposure of IOVs to the nucleotide. Effects on V_{max} require preincubation of IOVs in ATP for up to 10–15 min. The effects of ATP on the K_m for D-glucose efflux from IOVs are reversed by one wash of ATP-treated IOVs in ATP-free medium, but the reduced V_{max} for sugar efflux remains depressed following this treatment (D. N. Hebert and A. Carruthers, unpublished observations).

Discussion

Human red cell sugar transport is believed to be mediated via a 55-kDa integral membrane glycoprotein (band 4.5 protein; Kasahara & Hinkle, 1977; Baldwin et al., 1979; Pessin et al., 1984; Mueckler et al., 1985). This study demonstrates that the substrate-induced quenching of purified band 4.5 protein tryptophan fluorescence [i.e., quenching by sugars, cytochalasin B, phloretin, and ATP; see Carruthers (1986)] is also quantitatively reproduced in studies with red cell membranes lacking peripheral proteins. These findings add additional support to the view that a component of band 4.5 protein is the red cell sugar transport protein. These studies are also interesting for they indicate that one possible source of anomaly in red cell sugar transport kinetics [for a review, see Naftalin & Holman (1977)] could derive from the interaction of the transporter with ATP.

Naftalin and Holman (1977) and Widdas (1980) summarize the basic features of human erythrocyte hexose transfer. These are asymmetry in Michaelis and velocity constants for net efflux and influx, high K_m for zero-trans sugar efflux (efflux into sugar-free medium) but low K_m for infinite-trans exit (efflux into saturating levels of sugar), and high V_{max} and K_m for equilibrium exchange sugar fluxes ([D-glucose$_i$] = [D-glucose$_o$]). The gated-pore model of Naftalin and Holman (1977) accounts for these features but predicts that removal of intracellular hemoglobin results in a reduced K_m for zero-trans exit, little change in the K_m for zero-trans entry, and an increased V_{max} for entry. Upon removal of hemoglobin (and other cellular contents) by forming ghosts, the K_m for protein-mediated zero-trans exit falls (Carruthers & Melchior, 1983a; also see this study), the K_m for zero-trans entry increases (Jung et al., 1971; Taverna & Langdon, 1973; Carruthers & Melchior, 1983a; Carruthers, 1986; also see this study), and the V_{max} for sugar entry increases (Jung et al., 1971; Taverna & Langdon, 1973; Carruthers & Melchior, 1983a; Carruthers, 1986; also see this study). The net effect is symmetry in Michaelis and velocity constants for sugar transport. On the basis of the general concensus that the K_m for entry increases in ghosts, the gated pore model of Naftalin and Holman (1977) must be rejected.

This present study confirms and extends the earlier observations by demonstrating that although protein-mediated D-glucose transport in substantially hemoglobin-free red cell ghosts and IOVs is symmetric with respect to K_m and V_{max} parameters, asymmetry can be restored upon exposure of the normally endofacial surface of the plasma membrane to ATP. This is consistent with the finding that ATP reduced K_m and V_{max} for sugar efflux from IOVs (Carruthers, 1986). Jacquez (1983) has shown that ATP depletion of red cells by exposure to A 23187 and Ca^{2+} or to metabolic inhibitors reduces the V_{max} for sugar uptake at 5 °C. Moreover, V_{max} was restored upon forming ATP-containing ghosts from depleted cells. However, Jacquez did not find that K_m and V_{max} increased upon ghost formation. The reasons for these discrepancies remain uncertain but may be related to the different temperatures employed in transport determinations [the kinetics of red cell sugar transport show a marked sensitivity to alterations in temperature; see Naftalin & Holman (1977)].

A number of fundamental observations must be reconciled by any model for human red cell hexose transfer. In intact cells, these are the following: (1) the asymmetry of zero-trans net sugar influx and efflux; (2) the existence of two operational efflux sites (K_m for unidirectional efflux into medium containing saturating levels of D-glucose = 2.8 mM; K_m for exit into sugar-free medium = 28 mM); (3) the high V_{max} for unidirectional equilibrium exchange sugar fluxes ([D-glucose$_i$] = [D-glucose$_o$]); (4) apparent one-site transport kinetics in which only one molecule of substrate may be bound to the transporter at any point in time (Krupka & Deves, 1981; Gorga & Lienhard, 1981). In ghosts and IOVs, these are the following: (5) the loss of asymmetry in net fluxes (K_m for both influx and efflux = 10 mM); (6) the loss of two operational transport sites at the cytoplasmic surface of the membrane; (7) the presence of low and high app K_d substrate binding sites (K_l and K_h, respectively) detected in fluorescence quenching studies; (8) the ability of ATP to restore the anomolous asymmetric kinetics of sugar transport in ghosts and IOVs (Carruthers, 1986; see also here).

A critical starting point for any model relates to the question of whether the ternary complex of carrier–intracellular sugar–extracellular sugar (the two-site carrier) exists or whether the occupation of a substrate binding site by sugar excludes the possibility of occupation of a second site by substrate (the one-site carrier).

The sugar-induced fluorescence quenching data of this study may be used to determine whether two sugar binding sites exist simultaneously in stripped membrane preparations or whether occupancy of these sites by substrate is mutually exclusive (i.e., only one site can be occupied at any point in time). The one-site model may be simply described by the scheme shown in Figure 7A where X is unoccupied carrier, G_o is external sugar, G_i is internal sugar, and αq and βq represent quenching produced by the XG_i and XG_o complexes. For a nontransported sugar (e.g., ethylidene glucose or maltose), sugar-induced quenching, q, is described by

$$q = \frac{Q_m[S](\alpha + \beta K_A/K_B)}{K_A(1 + [S]/K_B) + [S]} \quad (1)$$

where Q_m is the maximal theoretical quenching and S replaces G_i and G_o (the stripped membranes are freely permeable to

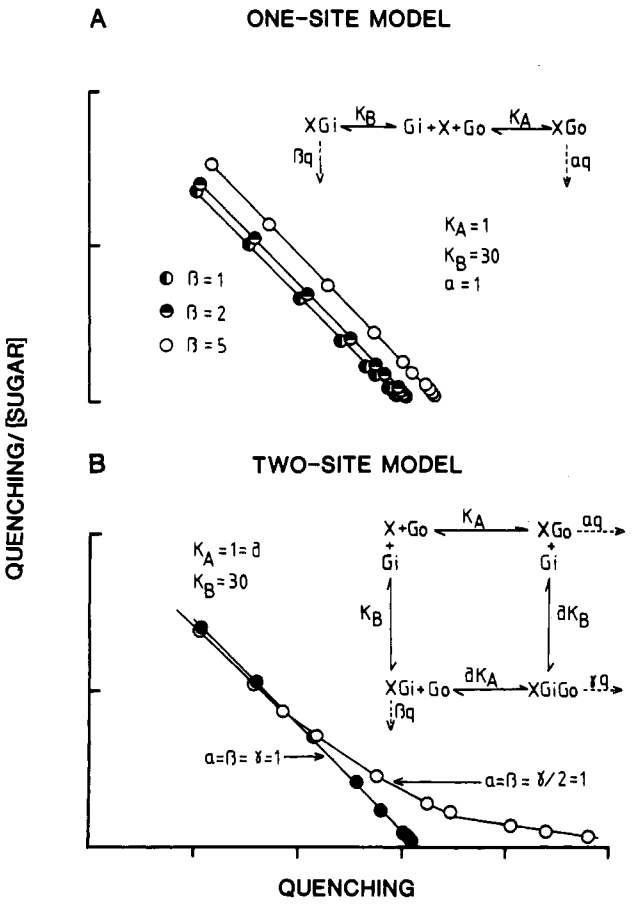

FIGURE 7: One- and two-site models for sugar-induced quenching of transporter fluorescence. (A) The one-site model. For nontransported sugars (e.g., maltose and ethylidene glucose), internal sugar and external sugar compete for occupation of the sugar binding site. The occupation of X by G_i excludes occupation by G_o and vice versa. Quenching by $G_o = \alpha q[XG_o]$, and quenching by $G_i = \beta q[XG_i]$. The equation describing this kinetic scheme is given in the text (see Discussion). K_A, K_B, and α values of 1, 30, and 1, respectively, were inserted (q is an arbitrary, fixed value), and β was varied. A series of parallel lines is predicted for Eadie/Scatchard plots. (B) The two-site model. With this scheme, the transporter X can be occupied simultaneously by G_o and G_i. Quenching is given by $\alpha q[XG_o] + \beta q[XG_i] + \gamma q[XG_iG_o]$. The equation describing this kinetic scheme is given in the text (see Discussion). K_A, K_B, α, β, and δ values of 1, 30, 1, 1, and 1 were inserted, and γ was varied. When $\alpha = \beta = \gamma$, a single straight line is predicted for Eadie/Hofstee plots of quenching data. When $\gamma > 1$, two-component quenching kinetics are observed. Similarly, if $\gamma = 1$ and $\delta > 1$, two-component quenching kinetics are observed (not shown). The experimental data cannot be used in their current form to distinguish between two identical sites with strong negative cooperativity ($\gamma = 1$, $\delta > 1$, $K_A = K_B$) or two noninteracting, different sites ($\gamma > 1$, $\delta = 1$, $K_A < K_B$).

sugar; therefore, both sides of the membrane are exposed to sugar simultaneously).

With the two-site model, the scheme shown in Figure 7B applies. For a nontransported sugar, quenching is described by

$$\frac{Q_m[S](\alpha + \beta K_A/K_B + \gamma[S]/dK_B)}{K_A(1 + [S]/K_B) + [S](1 + [S]/dK_B)} \quad (2)$$

Figure 7 illustrates the predictions of both one-site and two-site models. K_A and K_B values of 1 and 30 mM were substituted into these equations, and the parameters β and γ of eq 1 and 2, respectively, were varied. The one-site model is dominated by K_A, and, even if β is increased ($\beta > \alpha$; i.e., quenching produced by XG_i is greater than that produced by XG_o), a series of parallel lines in Eadie/Scatchard plots is predicted with no indication of two-component kinetics. With the two-site model, when $\alpha = \beta = \gamma$ (i.e., quenching produced by formation of XG_o, XG_i, and XG_oG_i is identical), a single straight line is predicted. When $\gamma > \alpha = \beta$ (i.e., quenching resulting from the formation of $XG_oG_i > XG_o = XG_i$), two-component Hofstee plots are produced. Provided that multiple sugar binding enzymes are not responsible for the stripped membrane results, these considerations permit us to reject the one-site model for substrate binding to the transporter. As these results have also been obtained by using purified sugar transporter in which the number of cytochalasin B binding proteins (i.e., proteins with the high app K_d binding site) comprised more than 80% of the total protein present and the number of phloretin binding proteins (i.e., proteins containing the low app K_d binding site) also comprised more than 80% of the total protein present [band 4.5 protein; see Carruthers (1986)], it is not unreasonable to conclude that rejection of the one-site model is justified.

Two previous studies have examined this question by two methods. Krupka and Deves (1981) modeled inhibitions of simple one-site and two site carrier systems produced by competitive inhibitors of transport that bind to either intra- or extracellular sugar binding sites. They concluded that their experimental data were consistent with the one-site model only (i.e., the ternary complex did not exist). However, they point out that should a trans-inhibitor fail to impede the binding of substrate to its cis binding site and should the ternary complex of transporter–cis and trans-inhibitor fail to be found, then their conclusions would be invalidated. These results would be in keeping with the ability of cytochalasin B to act as a competitive inhibitor of sugar exit and a noncompetitive inhibitor of entry and phloretin to act as a competitive inhibitor of entry but a noncompetitive inhibitor of exit (Krupka & Deves, 1981). This present study suggests that substrate occupation of a trans site in a two-site system is unaffected by occupancy of the cis site by inhibitor. Sogin and Hinkle (1980) have shown that phloretin inhibits cytochalasin B binding to purified transporter, indicating that the ternary complex of transporter–cis and trans-inhibitor is not found. The arbitrary restrictions that are necessary to reject the conclusions of Krupka and Deves (1981) are, therefore, observed experimentally, and we must conclude that their study does not exclude the two-site model.

Gorga and Lienhard (1981) employed a different approach to this problem. They monitored cytochalasin B binding to stripped ghost membranes in the presence of sugars that bind preferentially either to internal or to external substrate binding sites. They concluded that the ternary complex (transporter–cis and trans-sugar) is not found and that the two-site model must be rejected. However, their conclusions were based in part upon the assumption that the nontransported glucose analogue ethylidene glucose reacted solely with the external sugar binding site. The app K_i for ethylidene glucose inhibition of cytochalasin B binding to transporter was 26 mM—a value very close to that observed in this study (28 mM). They concluded that occupancy of the influx site by ethylidene glucose blocks occupancy of the internal (efflux) site by cytochalasin B. It is shown in this study, however, that ethylidene glucose reacts with the internal site with an app K_d of 28 mM and with the external site with an app K_d of 1.1 mM. Their findings are, therefore, also consistent with the view that occupancy of the external site has no effect on cytochalasin B binding to the internal site and that the observed competitive inhibition of cytochalasin B binding by ethylidene glucose is mediated via competition for binding solely at the internal site.

Table III: Predictions of Modulated Two-Site Random Carrier Model

	observed				predicted			
	intact cells		ghosts		2 nM ATP		0 ATP	
	K_m[a]	V_m[b]	K_m[a]	V_m[b]	K_m[a]	V_m[b]	K_m[a]	V_m[b]
zero-trans entry	1.6	36	10	185	4	40	10	200
zero-trans exit	25	190	10	194	20	200	10	200
infinite-cis entry	2.8	40	11	191	4.4	50	12	200
infinite-cis exit	1.8	185	11	198	1.6	200	12	200
equilibrium exchange	31	310			9	300	18	300
	12[c]	360[c]	21[d]	300[d]				

[a] In millimolar. [b] In millimoles per liter of cell water per minute. [c] Data taken from Weiser et al. (1983) for freshly drawn red cells. [d] Data taken from Weiser et al. (1983) for red cells stored in the cold for 8 weeks. The predicted values were calculated from the relationship influx

$$V_i = \frac{\frac{k_1[G_o]}{K_A} + \frac{k_2[ATP][G_o]}{\beta K_N K_A} + \frac{k_5[G_o][G_i]}{\alpha K_A K_B} + \frac{k_6[ATP][G_o][G_i]}{\beta\gamma\delta K_N K_A K_B}}{1 + \frac{[G_o]}{K_A} + \frac{[G_i]}{K_B} + \frac{[ATP]}{K_N} + \frac{[G_i][G_o]}{\alpha K_A K_B} + \frac{[ATP][G_i]}{\gamma K_B K_N} + \frac{[ATP][G_o]}{\beta K_N K_A} + \frac{[ATP][G_i][G_o]}{\beta\gamma\delta K_N K_A K_B}}$$

where the various translocation and dissociation constants are illustrated in Figure 8. Efflux is obtained by interchanging $k_1 \leftrightarrow k_3$, $k_2 \leftrightarrow k_4$ and, in terms lacking $[G_i]$, $[G_o] \leftrightarrow [G_i]$, $K_A \leftrightarrow K_B$, and $\beta \leftrightarrow \gamma$ in the numerator. The values employed as a first approximation were $k_1 = k_3 = k_4 = 200$, $k_5 = k_6 = 300$, and $k_2 = 40$ mmol (L of cell water)$^{-1}$ min^{-1}. $K_A = K_B = 10$ mM, and $\alpha = 1$, $\beta = 0.4$, $\gamma = 2$, and $\delta = 0.25$. For a passive transfer system in the absence of ATP, $K_A/K_B = k_1/k_3$, and in the presence of ATP, $\beta K_A/\gamma K_B = k_2/k_4$.

This is consistent with the results reported here indicating that ethylidene glucose competitively inhibits cytochalasin B binding to stripped membranes with an app K_i close to the high app K_d for binding to transporter. The low app K_d for ethylidene glucose binding was unaffected by the presence of cytochalasin B. This current study, therefore, supports the view that the ternary complex of transporter–external sugar–cytochalasin B is found and that cytochalasin B binding is unaffected by the occupancy of the external substrate binding site by sugar. These considerations permit the development of a two-site model for human red cell transport.

The proposed model incorporates the minimum number of steps necessary to predict the properties of red cell sugar transport and has the following features (see Figure 8). (1) In the absence of ATP, the transporter exists in four forms—X, G_o·X, X·G_i, and G_o·X·G_i where X is transporter and G_o and G_i refer to external and internal sugar, respectively. (2) In the absence of ATP, G_o and G_i interact with the binary complexes of X·G_i and G_o·X noncooperatively. (3) The ternary complex G_o·X·G_i undergoes reaction to form products more rapidly than G_o·X and X·G_i which are only partly reactive. (4) In the presence of ATP, four additional forms of carrier exist—X·ATP, X·ATP·G_i, G_o·X·ATP, and G_o·X·ATP·G_i. No assumptions are made regarding the mechanism of ATP action. ATP may modify sugar transport via allosteric interaction with the transporter or via γ-phosphoryl transfer to site(s) on the transporter [e.g., see Witters et al. (1986)] or to other proteins that interact with the transporter. (5) ATP has a negative cooperative effect on G_i binding to X, a positive cooperative effect on G_o binding to X, and a positive cooperative effect on G_o and G_i binding to the ternary complexes X·ATP·G_i and G_o·ATP·X, respectively. (6) The ternary complex G_o·X·ATP is less reactive than its ATP-free counterpart (G_o·X), is less reactive than X·ATP·G_i (which has equal reactivity to X·G_i), and, as with the nucleotide-free ternary complex, G_o·X·G_i, G_o·X·ATP·G_i is more reactive than G_o·X·ATP and X·ATP·G_i. This is a complex kinetic scheme which, if analyzed without making the rapid equilibrium assumption, would be of the hybrid ping-pong random type (Segel, 1975) including a central random Bi-Bi segment (to account for exchange fluxes) and two ordered Uni-Uni segments (to account for zero-trans fluxes). Moreover, the model would require additional steps resulting from the transporter's reaction with ATP. For this reason, a first approximation of the model's properties has been produced assuming rapid equilibrium kinetics (Figure 8) in which only catalytic (translocation) steps are rate limiting. Note, however, that in order to account for the wide differences between the app K_d parameters for sugar binding to transporter and the K_m parameters for transport, significant segments of the reaction must not be of the rapid equilibrium type, hence, this analysis of the model is not complete. Table III summarizes the predicted kinetic parameters of sugar transport in the presence and absence of ATP and those observed in intact cells and ghosts.

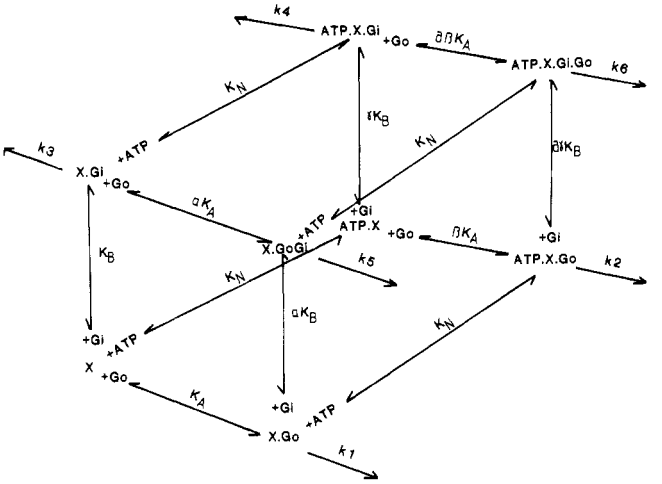

FIGURE 8: Model for ATP control of sugar transport in red cells. The carrier X can combine with G_o, G_i, and ATP to form the various complexes shown. Sugar binding sites for G_o and G_i exist simultaneously. The rate-limiting steps for efflux, influx, and exchange fluxes (translocation) are given rate constants k_3 and k_4, k_1 and k_2, and k_5 and k_6, respectively. The reaction with ATP (X + ATP $\leftrightarrow$ X·ATP) should not be interpreted literally. It is not currently known whether ATP modifies the transporter's properties via allosteric or covalent (phosphorylation) mechanisms.

The model predicts symmetry in zero-trans Michaelis and velocity parameters in ghosts and asymmetry in zero-trans kinetics in the presence of ATP and the presence of two operational Michaelis parameters for sugar efflux in the presence of ATP (zero-trans efflux K_m > infinite-trans exit K_m). The major discrepancy between predicted and experimental behavior arises in the equilibrium exchange procedure where the model predicts a K_m for D-glucose exchange of about 9 mM

in the presence of ATP and 18 mM in the absence of ATP. The accepted value for exchange D-glucose transport in intact red cells is 30 mM [see Naftalin & Holman (1977)]. Recently, however, Weiser et al. (1983) reported that the K_m for exchange D-glucose transport in freshly drawn intact red cells at 20 °C is 12 mM and for exchange transport in 8-week cold-stored blood is 21 mM. These values are not very different from those predicted for the two-site transporter (±ATP) and provide corroborative (but not direct) support for the model. Any effects of ATP on transport would, according to the model, be amplified in the exchange condition. The ATP-sensitive two-site model is, therefore, the simplest model that accounts for and mimics quantitatively most of the observed red cell and red cell ghost transport data, although this, in itself, does not discount the possibility that other, more complex models could also mimic the behavior of the transport system.

Conclusions

Sugar transport in human red cells is modulated by ATP. The molecular mechanism of ATP action remains to be defined, but the net effect of the nucleotide is to alter the apparent kinetics of substrate binding to the transport protein. Two substrate binding sites have been detected in fluorescence quenching experiments—one with high affinity for transported and nontransported sugars and the other with low affinity. These sites correspond in all probability to the influx and efflux sites on the transporter and substantially confirm the view that the sugar transport system is intrinsically asymmetric with respect to substrate binding constants (Wheeler & Hinkle, 1985). Occupation of these sites by substrate is not mutually exclusive. The available evidence supports the view that transport in ATP-free ghosts and inside-out vesicles is symmetric. This apparent contradiction (asymmetry vs. symmetry) is easily reconciled if the transport system is not of the rapid equilibrium type; i.e., asymmetric binding constants are compensated by asymmetric translocation constants resulting in apparent symmetry of transport. Addition of ATP to ghosts restores transport asymmetry and the two operational sugar transport sites at the interior of the cell. Moreover, the asymmetry in substrate binding constants detected in fluorescence quenching studies is further exaggerated by ATP. A model is proposed that can account for most of the features of red cell sugar transport. This model assumes two sugar binding sites can exist simultaneously and that ATP modifies both the substrate affinities and catalytic reactivities of the various transporter–substrate complexes.

While red cell sugar transport is not considered to be regulated in a classical sense, these findings may be of some significance to transport in muscle. Sugar transport in skeletal muscle is stimulated by insulin, metabolic depletion, and contractile activity [see Carruthers (1984)]. Insulin appears to stimulate transport via a recruitment mechanism similar to that found in adipose (Wardzala & Jeanrenaud, 1983; Cushman & Wardzala, 1980; Suzuki & Kono, 1980; Kono et al., 1981). In adipose tissue, insulin-stimulated carrier recruitment is an energy-dependent phenomenon (Kono et al., 1981). It seems unlikely, therefore, that metabolic depletion stimulates sarcolemmal sugar transport via a recruitment-type mechanism. It is possible, however, that as with the red cell, ATP interacts directly with plasmalemmal transporters to alter their intrinsic activity. The studies of Baker and Carruthers (1981a,b, 1983, 1984) and Simons (1983a,b) are consistent with this view and substantially support the hypothesis of Randle and Smith (1958) that membrane sugar transport is controlled by the phospho content of the transport molecule or molecules regulating transporter function.

Acknowledgments

I thank Dr. S. Sarikas for performing electron microscopy on inside-out vesicles and C. Rodgers for his excellent work in the design and manufacture of the stirring apparatus used in this study.

Registry No. ATP, 56-65-5; AMP, 61-19-8; ADP, 58-64-0; AMP-PCP, 3469-78-1; AMP-CPP, 7292-42-4; Ap_4A, 5542-28-9; DG, 50-99-7; 2-deoxy-DG, 154-17-6; 3-*O*-Me-DG, 146-72-5; EG, 13224-99-2; D-galactose, 59-23-4; maltose, 69-79-4; cytochalasin B, 14930-96-2; pholoretin, 60-82-2.

References

Applemen, J. R., & Lienhard, G. E. (1985) *J. Biol. Chem. 260*, 4575–4578.
Baker, G. K., & Naftalin, R. J. (1979) *Biochim. Biophys. Acta 550*, 474–484.
Baker, P. F., & Carruthers, A. (1981a) *J. Physiol. (London) 316*, 481–502.
Baker, P. F., & Carruthers, A. (1981b) *J. Physiol. (London) 316*, 503–525.
Baker, P. F., & Carruthers, A. (1983) *J. Physiol. (London) 336*, 397–431.
Baker, P. F., & Carruthers, A. (1984) *Curr. Top. Membr. Transp. 22*, 91–103.
Baldwin, S. A., Baldwin, J. M., Gorga, F. R., & Lienhard, G. E. (1979) *Biochim. Biophys. Acta 552*, 183–189.
Baldwin, S. A., Baldwin, J. M., & Lienhard, G. E. (1982) *Biochemistry 21*, 3836–3842.
Batt, E. P., Abbott, R. E., & Schacter, D. (1976) *J. Biol. Chem. 251*, 7184.
Benes, I., Kolinska, J., & Kotyk, A. (1972) *J. Membr. Biol. 8*, 303–309.
Burstein, E. A., Vedenkina, N. S., & Ivkova, M. N. (1973) *Photochem. Photobiol. 18*, 263–279.
Carruthers, A. (1984) *Prog. Biophys. Mol. Biol. 43*, 33–69.
Carruthers, A. (1986) *J. Biol. Chem.* (in press).
Carruthers, A., & Melchior, D. L. (1983a) *Biochim. Biophys. Acta 728*, 254–266.
Carruthers, A., & Melchior, D. L. (1983b) *Biochemistry 22*, 5797–5807.
Carruthers, A., & Melchior, D. L. (1984) *Biochemistry 23*, 2712–2718.
Carruthers, A., & Melchior, D. L. (1985) *Biochemistry 24*, 4244–4250.
Challiss, J. R. A., Taylor, L. P., & Holman, G. D. (1980) *Biochim. Biophys. Acta 602*, 155–166.
Chen, R. F. (1981) *Anal. Lett. 14*, 1591–1601.
Cushman, S. W., & Wardzala, L. J. (1980) *J. Biol. Chem. 255*, 4755–4762.
Duggleby, R. G. (1981) *Anal. Biochem. 110*, 9–18.
Foster, D. M., Jacquez, J. A., Lieb, W. R., & Stein, W. D. (1979) *Biochim. Biophys. Acta 555*, 349–351.
Ginsberg, H., & Stein, W. D. (1975) *Biochim. Biophys. Acta 382*, 353–368.
Gorga, F. R., & Lienhard, G. E. (1981) *Biochemistry 20*, 5108–5113.
Gorga, F. R., & Lienhard, G. E. (1982) *Biochemistry 21*, 1905–1908.
Hanahan, M. F., & Jacquez, J. A. (1978) *Membr. Biochem. 1*, 239.
Hankin, B. C., Lieb, W. R., & Stein, W. D. (1972) *Biochim. Biophys. Acta 288*, 114–126.
Harris, E. J. (1964) *J. Physiol. (London) 173*, 344–353.
Jacquez, J. A. (1983) *Biochim. Biophys. Acta 727*, 367–378.

Jarvis, S. M., & Young, J. D. (1981) *Biochem. J. 194*, 331–338.
Jung, C. Y., & Rampal, A. L. (1977) *J. Biol. Chem. 252*, 5456–5463.
Jung, C. Y., Carlson, L. M., & Whaley, D. A. (1971) *Biochim. Biophys. Acta 241*, 613–627.
Kasahara, M., & Hinkle, P. C. (1977) *J. Biol. Chem. 253*, 7384–7390.
Kono, T., Suzuki, K., Dansey, L. E., Robinson, F. W., & Blevins, T. L. (1981) *J. Biol. Chem. 256*, 6400–6407.
Krupka, R. M., & Deves, R. (1981) *J. Biol. Chem. 256*, 5410–5416.
Lieb, W. R., & Stein, W. D. (1974) *Biochim. Biophys. Acta 373*, 178–196.
Lin, S., & Snyder, C. E., Jr. (1977) *J. Biol. Chem. 252*, 5464–5471.
Lowry, O. H., Rosebrough, N. J., Farr, A. L., & Randall, R. (1951) *J. Biol. Chem. 193*, 265–275.
Naftalin, R. J., & Holman, G. D. (1977) in *Membrane Transport in Red Cells* (Eellory, J. C., & Lew, V. W., Eds.) pp 257–300, Academic Press, New York.
Naftalin, R. J., & Roselaar, S. E. (1985) *J. Physiol. (London) 365*, 88P.
Parker, C. A. (1968) *Photoluminescence of Solutions*, p 222, American Elsevier, Amsterdam.
Pessin, J. E., Tillotson, L. G., Isselbacher, K. J., & Czech, M. P. (1984) *Fed. Proc., Fed. Am. Soc. Exp. Biol. 43*, 2258–2261.
Randle, P. J., & Smith, G. H. (1958) *Biochem. J. 70*, 501–509.
Rich, G. T., Sha'afi, R. I., Romualdez, A., & Solomon, A. K. (1968) *J. Gen. Physiol. 52*, 941–954.
Segel, I. H. (1975) in *Enzyme Kinetics*, Wiley, New York.
Sen, A. L., & Widdas, W. F. (1962) *J. Physiol. (London) 160*, 392–403.
Shelton, R. L., & Langdon, R. G. (1983) *Biochim. Biophys. Acta 733*, 25–33.
Simons, T. J. B. (1983a) *J. Physiol. (London) 338*, 477–500.
Simons, T. J. B. (1983b) *J. Physiol. (London) 338*, 501–526.
Sogin, D. C., & Hinkle, P. C. (1980) *Biochemistry 19*, 5417–5420.
Spears, G., Sneyd, J. G. T., & Loten, E. G. (1971) *Biochem. J. 125*, 1149–1151.
Speizer, L., Haugland, R., & Kutchai, H. (1985) *Biochim. Biophys. Acta 815*, 75–84.
Suzuki, K., & Kono, T. (1980) *Proc. Natl. Acad. Sci. U.S.A. 77*, 2542–2545.
Taverna, R. D., & Langdon, R. G. (1973) *Biochim. Biophys. Acta 298*, 422–428.
Torikata, T., Forster, L. S., O'Neal, C. C., Jr., & Rupley, J. A. (1979) *Biochemistry 18*, 385–390.
Viera, F. L., Sha'afi, R. I., & Solomon, A. K. (1970) *J. Gen. Physiol. 55*, 451–466.
Wardzala, L. J., & Jeanrenaud, B. (1983) *Biochim. Biophys. Acta 730*, 49–56.
Weiser, M. B., Razin, M., & Stein, W. D. (1983) *Biochim. Biophys. Acta 727*, 379–388.
Wheeler, T. J., & Hinkle, P. C. (1985) *Annu. Rev. Physiol. 47*, 503–517.
Widdas, W. F. (1952) *J. Physiol. (London) 118*, 23–39.
Widdas, W. F. (1980) *Curr. Top. Membr. Transp. 14*, 165–223.